Archives of Pharmaceutical Sciences Ain Shams University 2021; Vol. 5(2): 354-370

OPEN ACCESS

Biochemistry

Research Article

Nephroprotective Role of Combined Sitagliptin and Oleuropein in Cisplatin-Induced Acute Kidney Injury: Regulation of SDF-1α/Nrf2/HO-1 Axis and Autophagy

Mohamed Bassiony[a], Nesreen N. Omar[a], Amira M. Badr[b,c], Nadia M. Hamdy[d], Eman F. Sanad[d*]

[a]*Department of Biochemistry, Faculty of Pharmacy, Modern University for Technology and Information, Cairo, Egypt*
[b]*Department of Pharmacology and Toxicology, Faculty of Pharmacy, Ain Shams University, Cairo 11566, Egypt*
[c]*Department of Pharmacology and Toxicology, Faculty of Pharmacy, King Saud University, Riyadh, Saudi Arabia*
[d]*Department of Biochemistry, Faculty of Pharmacy, Ain Shams University, Cairo 11566, Egypt*

ABSTRACT

Accumulating evidence proves that cisplatin, a widely used anticancer, causes acute kidney injury (AKI). Sitagliptin (Sita), a dipeptidyl peptidase-4 (DPP4) inhibitor, is a hypoglycemic agent that can promote tissue angiogenesis and cell survival. However, little is known about the nephroprotective effect of Sita in cisplatin-induced AKI especially its effect on SDF-1α, usually degraded by DPP4. Meanwhile, the olive oil component oleuropein (Ole) activates Nrf2/heme oxygenase-1 (HO-1) axis, which ultimately leads to SDF-1α activation. Herein, we studied the nephroprotective effects of combined Sita and Ole on oxidative stress and autophagy through SDF-1α/Nrf2/ HO-1 axis in cisplatin-induced AKI in rats. AKI was induced *in vivo* through single IP injection of cisplatin (7 mg/kg), while Sita (10 mg/kg) and Ole (16 mg/kg) were given separately and in combination for 7 days prior and 5 days after cisplatin injection. AKI was assessed through histopathological examination, measurement of serum creatinine and urea. Also, serum GLP-1, serum and kidney SDF-1α levels were measured by ELISA. LC3-II, P62, HO-1, Nrf2, and caspase-3 were investigated by western blotting. Sita and Ole monotherapy and in combination accelerated kidney recovery as they suppress serum SDF-1α, serum BUN, creatinine and renal histopathological features. Each of Sita and Ole enhanced Nrf2/HO-1axis in renal tissues while only Sita enhanced renal SDF-1α. Sita and Ole monotherapy showed incompetent autophagy where the late steps of autophagy were incomplete. Combined treatment enhanced SDF-1α in kidney tissue which showed recovery through autophagy process. In conclusion**,** Sita and Ole show promising nephroprotective effects in cisplatin-induced AKI.

Keywords: *Cisplatin; Acute Kidney Injury; Sitagliptin; Oleuropein; SDF-1α; Nrf2; Autophagy; Caspase-3*

***Correspondence** | Eman F. Sanad; Department of Biochemistry, Faculty of Pharmacy, Faculty of Pharmacy, Ain Shams University, Cairo 11566, Egypt. Email: dr.emansanad@pharma.asu.edu.eg

Citation | Bassiony M, Omar NN, Badr AM, Hamdy NM, Sanad EF, 2021. Nephroprotective Role of Combined Sitagliptin and Oleuropein in Cisplatin-Induced Acute Kidney Injury: Regulation of SDF-1α/Nrf2/ HO-1 Axis and Autophagy. Arch Pharm Sci ASU 5(2): 354-370
DOI: 10.21608/aps.2021.104714.1072

Print ISSN: 2356-8380. **Online ISSN**: 2356-8399.

Received 07 November 2021. **Accepted** 14 December 2021.

Published by: Ain Shams University, Faculty of Pharmacy

1. Introduction

Acute kidney injury (AKI) is a serious complication of hospitalized patients caused by a broad-spectrum of insults **[1]**. Kidneys are primarily targeted owing to excessive blood supply. Despite the use of various pharmacologic agents, the mortality rate is still 25-70% **[2]**. AKI arises in the form of a clinical syndrome, in which the structural damage associated with the injury is manifested as a rapid decline in glomerular filtration rate and disposal

of nitrogenous waste **[3]**.

Cisplatin-induced AKI in rats is an optimal animal model of AKI that is simple, reproducible, and closest to clinical situations **[4]**. Cisplatin is a platinum chemotherapeutic agent used in the management of a myriad of solid tumors, however nephrotoxicity barricaded against effective clinical application **[5]**. Being a small and uncharged molecule, cisplatin is freely filtered by the glomeruli after which it is uptaken by the proximal tubules **[6]**. Within renal cells, accumulated cisplatin is bioactivated into a savoring form which perpetrates mitochondrial dysfunction, DNA damage, and apoptosis **[7]**. An abundance of reactive oxygen species and inactive antioxidant systems are prompted by cisplatin in renal cells which contributes to a status of severe oxidative stress **[8]**. Altogether, cisplatin elicits intrinsic renal failure through direct tubular toxicity combined with acute vascular injury **[9]**. Undoubtedly, unmet oxygen and nutrient requirements due to vascular ischemia is exacerbated by increased energy demands caused by tubular cells stress. The failure to maintain energy homeostasis can be revamped by autophagy **[10]**. Autophagy is the fundamental process for cellular reconciliation during time of stress as it catabolizes damaged components so that they can be reused, boosting cell survival **[11]**.

To find a cure for acute kidney damage, pharmacological agents that confront cellular stress, while stimulating pro-survival pathways should be scrutinized. One of such candidates is sitagliptin (Sita), a selective dipeptidylpeptidase-4 (DPP4) inhibitor, used as a therapy for type II diabetes mellitus **[12]**. DPP-4 is an integral transmembrane protein located on the surface of cells in multiple organs including the kidneys **[13]**. DPP-4 inhibition impedes the exopeptidase activity of DPP-4 on glucagon-like peptide-1 (GLP-1) prolonging its action and maintaining normal glucose homeostasis **[14]**. Aside from the hypoglycemic action, Sita exhibited a putative role in tissues protection **[15]**. Interestingly, stromal cell-derived factor-1 (SDF-1α), another substrate for DPP-4, was found to promote cell survival through CXCR4 signaling **[16]**. Efficient SDF-1α/CXCR4 signaling can mobilize endothelial progenitor cells to form new blood vessels *in situ* through a process called vasculogenesis **[17]**. A new and broader niche of SDF-1α in local preservation of different organs is suggested **[18]**. The effect of Sita on serum and renal levels of SDF-1α is however unknown. Moreover, the impact of Sita on the autophagy response as a mechanism of renal repair in cisplatin toxicity is unclear.

On the other hand, olive leaf components showed anti-apoptotic, antioxidant, and neuroprotective properties **[19]**. Chiefly, oleuropein (Ole) plays a major role in improving mitochondrial function as it lessens oxidative stress by activating the nuclear factor-erythroid 2-related factor 2 (Nrf2) pathway which induces heme oxygenase-1 (HO-1) **[20]**. In the injury setting, Nrf2/HO-1 axis holds a great potential to be implicated with SDF-1α in a positive-feedback loop for therapeutic effects **[21]**. In this context, we hypothesize that Ole can synergize with Sita through SDF-1α/Nrf2/HO-1 panel in ameliorating cisplatin-induced AKI.

We aimed through this study to assess the nephroprotective effects of Sita as a synthetic DPP-4 inhibitor and novel natural antioxidant drugs as Ole and their combination on cisplatin-induced nephrotoxicity. In addition, we intended to measure intra-renal autophagy, apoptotic and oxidative stress markers as underlying mechanisms.

2. Materials and Methods

2.1. Drugs and chemicals

Oleuropein was purchased from Sigma-

Aldrich (Germany), Sitagliptin from MSD Pharmaceutical company (Egypt) and Cisplatin from Mylan pharmaceutical company (France). All other chemicals were of the highest purity grade commercially available.

2.2. Animals

All animal procedures and care were conducted according to the guidelines and the approval of the Research Ethics Committee of the Faculty of Pharmacy, Ain Shams University. Eighty male Sprague-Dawley rats (145-165 g) 6-8 weeks old were selected from the Animals Research Center in the Faculty of Medicine, Ain Shams University. Animal cages were air-conditioned with 22±2 °C temperature along with a 12 h light and dark cycle. They were given an acclimatization period of one week prior to the start of the experiment with free access to standard laboratory chow and tap water ad libitum.

2.3. Experimental design

Rats were randomly divided into 8 groups (10 rats per group); the 1st group (control group) received physiological 0.9% NaCl normal saline for 13 consecutive days; the 2nd group (Sita group) received sitagliptin (10 mg/kg, orally) for 13 days **[22]**; the 3rd group (Ole group) received oleuropein (16 mg/kg, orally) for 13 days **[23]**; the 4th group (Ole+Sita) received oleuropein (16 mg/kg, orally) and sitagliptin (10 mg/kg, orally) for 13 days; the 5th group (cisplatin group) injected with a single dose of cisplatin (7 mg/kg, intraperitoneal) after one week from the start of the experiment **[24]**; the 6th group (Cis/Sita group) received sitagliptin (10 mg/kg, orally) for 1 week before cisplatin injection and till the end of the experiment; the 7th group (Cis/Ole group) received oleuropein (16 mg/kg, orally) for 1 week before cisplatin injection and till the end of the experiment; the 8th group (Cis/Sita+Ole group) received both sitagliptin (10 mg/kg, orally) and oleuropein (16 mg/kg, orally) for 1 week before cisplatin injection and till the end of the experiment. Five days following the cisplatin injection, animals were sacrificed, and blood samples were collected. Centrifugation at 3000g for 10 min was carried out for serum separation. Then, and kidneys were excised and rinsed with ice-cold saline. Kidney tissues were homogenized in saline at ratio 1:10 (w/v), and the resulting homogenate was used in the subsequent biochemical analyses. Moreover, 10% buffered formalin or glutaraldehyde, was used to fix other renal specimens for histopathological and ultrastructural investigations.

2.4. Assessment of nephrotoxicity indices

Using commercial kits purchased from Bio-diagnostics company, Giza, Egypt. Serum creatinine, urea levels, alanine transferase (ALT) and aspartate transferase (AST) were assessed according to their standard procedures.

2.5. Histopathological examination

Renal tissue samples were fixed in formalin at a concentration of 10% and divided into paraffin segments of 4 μm thickness. Segments were dyed using hematoxylin and eosin (H&E).

2.6. Transmission Electron Microscopy

A part of each kidney was cut into small pieces (1 mm^3), treated with 2.5% glutaraldehyde 0.1 N PBS at room temperature for one hour, and then fixed with osmium tetraoxide for another hour. Renal tissues were dehydrated in 70, 90 and 100% acetone (twice) for five minutes each, then dehydrated in 1:1 (acetone:resin) for five minutes and then embedded in epoxy resin. Observation for ultrathin slices (90 nm) was done using a transmission electron microscope, Jeol Jem- 1400 (USA).

2.7. Assessment of oxidative stress markers

Rats' renal tissues were placed in normal saline and homogenized in a ratio of 1:9 (g):

(mL) in ice bath. The supernatant was removed after 15 min of centrifugation at 3000g under 4 °C. Superoxide dismutase (SOD) as well as Malondialdehyde (MDA) levels of renal tissues were assessed using commercial kits purchased from Bio-diagnostics, Giza, Egypt according to their standard procedures.

2.8. Assessment of GLP-1 and SDF-1α

Renal tissue GLP-1 levels were measured by Mouse Glucagon-like peptide-1 ELISA Kit (Bioassay Technology Laboratory, Shanghai, China). Both serum and renal tissue levels of SDF-1α were evaluated by Rat Stromal Cell Derived Factor 1α ELISA Kit (Finetest, Wuhan, China) according to their manufacturer's instructions.

2.9. Western Blot

Tissue protein was extracted using TRIzol reagent, and protein concentrations were estimated by the Bradford method. Equal amounts of protein per lane were separated with 10% SDS polyacrylamide gel electrophoresis gels and electrophoretically transferred to polyvinylidene difluoride membranes. Membranes were then incubated at room temperature for 2 h with blocking solution comprised of 5% non-fat dried milk in 10 mM Tris-Cl, pH 7.5, 100 mM NaCl, and 0.1% Tween 20. Membranes were incubated overnight at 4 ºC with 5.0 µg/mL (dilution of 1:1000) of the indicated primary antibodies against GAPDH, caspase-3, P62, LC3-II, Nrf2 and HO-1 (Santa Cruz Biotechnology inc, USA), and then incubated with a Rat anti-rabbit secondary monoclonal antibody conjugated to horseradish peroxidase at room temperature for 2 h. After each incubation, the membranes were washed four times with 10 mM Tris-Cl, pH 7.5, 100 mM NaCl, and 0.1% Tween 20 at room temperature. Chemiluminescence detection was performed with the Amersham detection kit according to the manufacturer's protocols. The amount of the studied protein was quantified by densitometric analysis using BioRad software, USA. Results were expressed as arbitrary units after normalization for GAPDH protein expression.

2.10. Statistical analysis

The data are represented as (mean ± SD). Statistical analyses were conducted using one-way ANOVA followed by Tukey-Kramer as a post-hoc test. Probability level equal to 0.05 is the criterion for significance. All statistical analyses were conducted by utilizing Instat version 3 software package. Graph Pad Prism (ISI® software, USA) version 8.4.3 software were utilized for drawing the graphs.

3. Results

3.1. Effect of cisplatin, sitagliptin and oleuropein on liver function and nephrotoxicity indices

AST and ALT levels were markedly higher in the cisplatin-intoxicated group indicating significant hepatic damage when compared with the control and treatment groups. Notably, the combined treatment group showed no significant difference in ALT and AST levels when compared with the control groups, indicating potential tissue protective effects **(Fig. 1A)**.

Biochemical assessment of serum nephrotoxicity markers showed that both serum creatinine and urea were markedly elevated in the cisplatin group when compared with the control and treatment groups. Treatment with sitagliptin and oleuropein alone showed significant alternations in these markers when compared with the cisplatin group but to a lesser extent than that of the combination group. There was no significant difference between the control group and the combined treatment group ($p>0.5$). It was also observed that kidney weight measurements of the cisplatin group were markedly higher than

those of the control and treatment groups **(Fig. 1B)**. There was no significant difference in kidney weight between the combined-treatment group and the control groups (p= 0.8238).

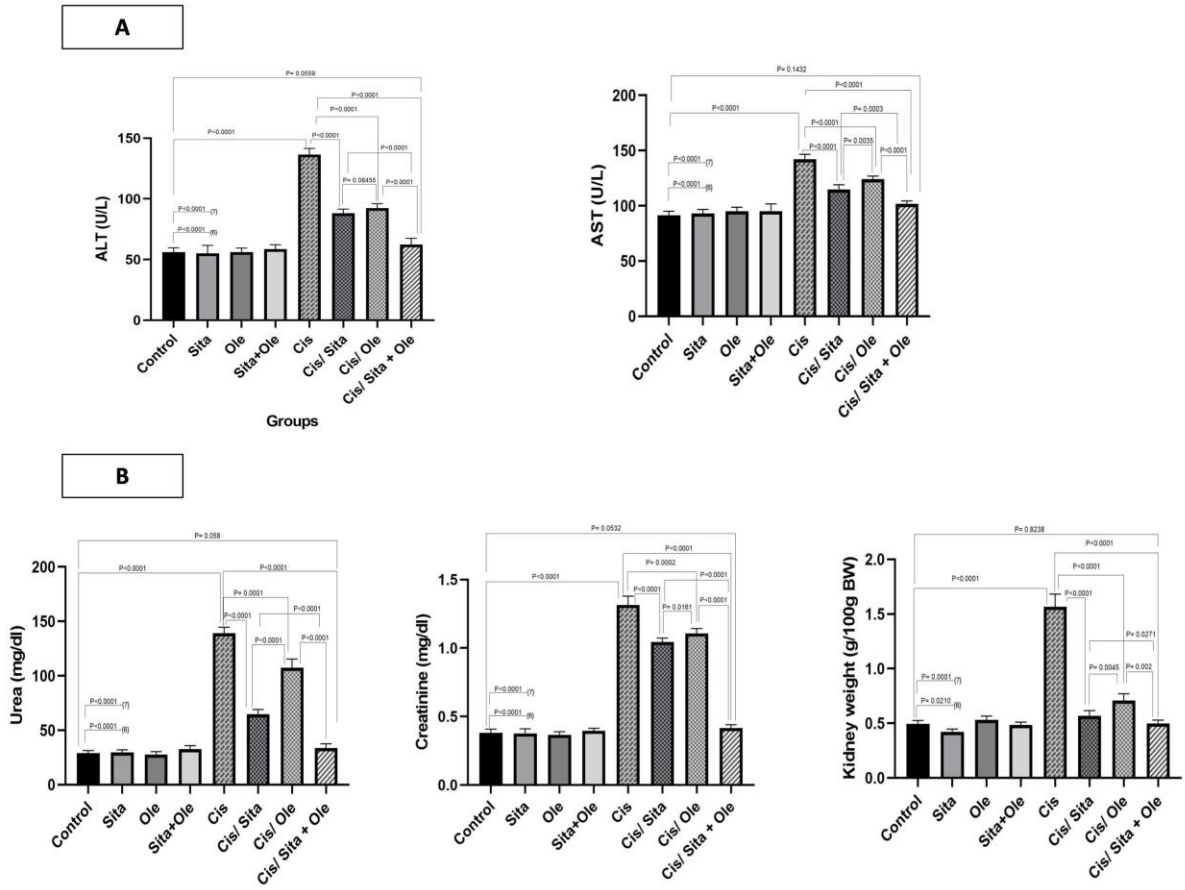

Fig. 1. Effect of cisplatin, sitagliptin, oleuropein and combination of them on liver functions **(A)** and nephrotoxicity indices **(B)**. Data are presented as means ± SD. P < 0.05 is considered statistically significant; one-way ANOVA followed by Bonferroni-corrected post hoc tests were performed.

3.2. Effect of sitagliptin and oleuropein on serum SDF-1α in cisplatin-treated rats

Serum SDF-1α has been considered as an early marker for tissue damage, as serum levels rise significantly after kidney injury to regulate the migration and proliferation of stem cells. It has also been documented to rise significantly after tissue damage in the kidneys, liver, bones, lungs and in ischemia. Accordantly, our results showed a significant increase in serum SDF-1α in the cisplatin-intoxicated group (2-fold) compared with the control groups **(Fig. 2A)**. Both sitagliptin and oleuropein as single treatment significantly lowered serum SDF-1α, while sitagliptin showed better results than oleuropein in their respective doses. Although serum SDF-1α in the combined-treatment group were significantly lower than the single-treatment groups, it was still significantly higher than the control groups (p= 0.039).

3.3. Effect of sitagliptin and oleuropein on tissue SDF-1α in cisplatin-treated rats

As serum SDF-1α is subjected to degradation by DPP-4 exopeptidases that are ubiquitously expressed on the surface of renal cells, only tissue levels of SDF-1α can be considered as a marker of renal rehabilitation and repair. Interestingly, tissue SDF-1α levels in the cisplatin group were significantly lower than those of the control groups and in contrast to serum levels. Sita administration enhanced the tissue levels of SDF-1α relative to the cisplatin group **(Fig. 2B)**. Oleuropein treatment showed a significant increase in tissue SDF-1α levels but still significantly lower than those of sitagliptin treatment. The highest levels of tissue SDF-1α were observed in the combined-treatment group suggesting potent renal tissue rehabilitation properties.

3.4. Effect of sitagliptin and oleuropein on tissue GLP-1 in cisplatin-treated rats

Our results showed no significant difference in tissue GLP-1 levels amongst the untreated control group, cisplatin-intoxicated group and/or the combined-treatment group. On the other hand, sitagliptin administration showed a significant increase in tissue GLP-1 levels either in the sitagliptin control group or the sitagliptin-treated group **(Fig. 2C)**.

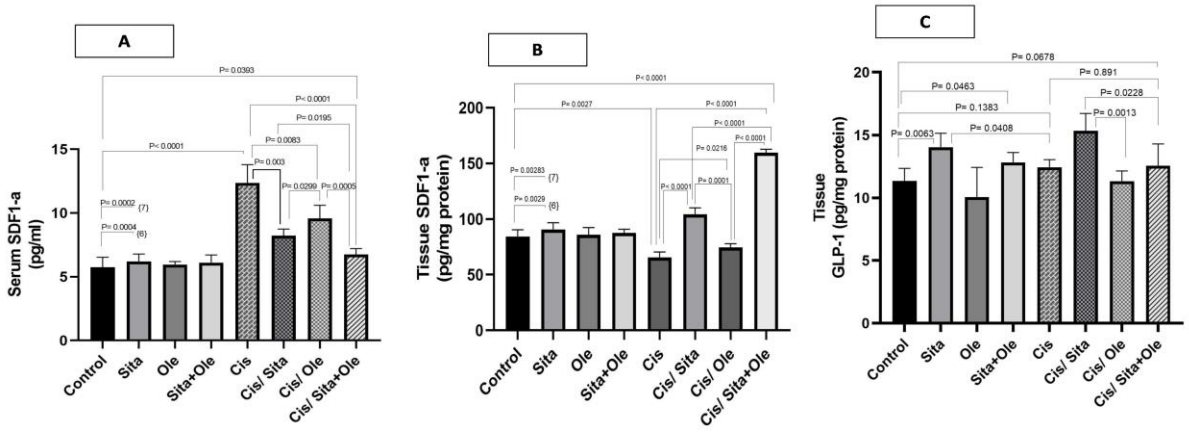

Fig. 2. Effect of cisplatin, sitagliptin, oleuropein and combination of them on some DPP4 substrates; **A:** SDF-1α in serum (pg/ml); **B:** SDF-1α in renal tissues (pg/mg protein); **C:** GLP-1 in renal tissues (pg/mg protein). Data are presented as means ± SD. P < 0.05 is considered statistically significant; one-way ANOVA followed by Bonferroni-corrected post hoc tests were performed.

3.5. Effect of sitagliptin and oleuropein on renal histology of cisplatin-treated rats

Histopathological examination of renal tissue showed normal glomerular **(Fig. 3, A-D)** and tubular cells **(Fig. 4, A-D)** architecture in the control and negative control groups. While renal tissues from cisplatin-intoxicated rats showed degenerated glomerular tufts **(Fig. 3E)**, hemorrhage, and atrophied tubules **(Fig. 4E)**. Pretreatment with Sita almost conserved the glomerular architecture **(Fig. 3F)** while renal tubular cells were incompletely recovered **(Fig. 4F)**. In the Ole group, both the glomerular **(Fig. 3G)** and tubular cells **(Fig. 4G)** were malformed. Coadministration of Sita and Ole considerably ameliorated the glomerular **(Fig. 3H)** and tubular damage **(Fig. 4H)**.

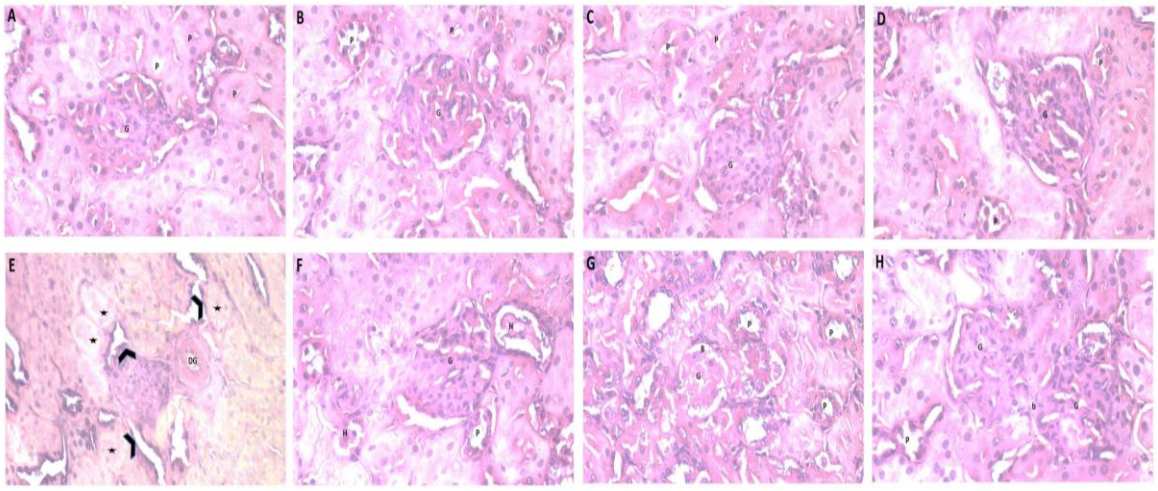

Fig. 3. Photomicrographs of histological sections of glomerular structure of rats' renal cortex by Hematoxylin and eosin. **A:** Control group; **B:** Negative control treated with sitagliptin; **C:** Negative control treated with oleuropein; **D:** Negative control treated with combination of sitagliptin and oleuropein, all can be seen with normal glomerular tuft (G), normal proximal convoluted tubules (P); **E**: Cisplatin treated rats have shrunken degenerated glomerular tuft (G) with abundant hemorrhage, atrophied tubules (stars). **F:** Cisplatin+sitagliptin treated rats show the regaining of the vasculature of the glomeruli and the architecture of the tubular cells which show rounded vesicular central nuclei, still there is an abundance of hyaline cast. **G**: Cisplatin+ oleuropein treated rats show shrunken glomerular tuft that has few nuclei and dilated Bowman's space (B), proximal tubular cells recovered their cubical cells and vesicular nuclei as well as lumen clear from cast. **H**: Cisplatin+ sitagliptin+ oleuropein treated group show Malpighian renal corpuscle containing glomerulus (G) and non- dilated Bowman's space (B), normal proximal convoluted tubules (P) with vesicular nuclei.

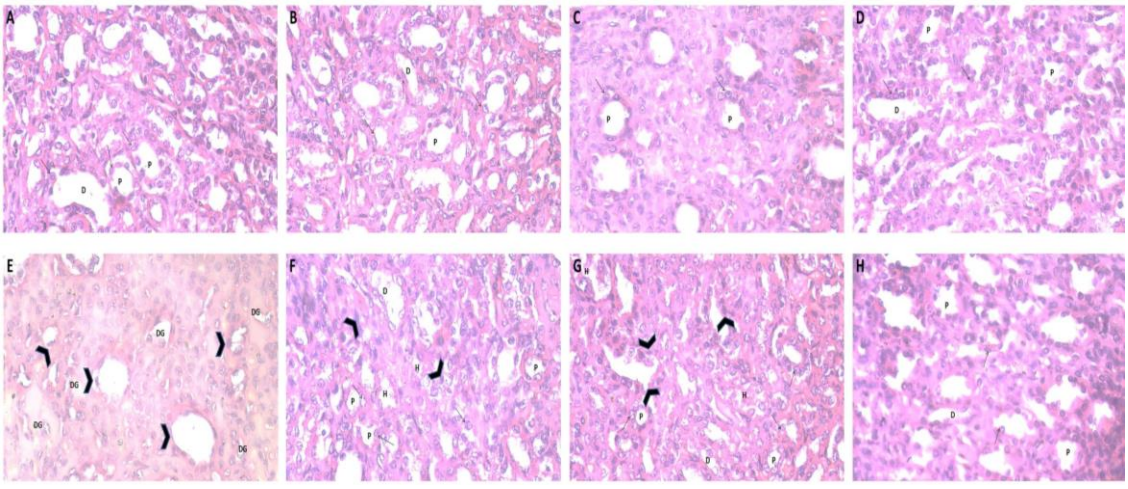

Fig. 4. Photomicrographs of histological sections of tubular structure of rats' renal cortex by Hematoxylin and eosin. **A:** Control group; **B:** Negative control treated with sitagliptin; **C:** Negative control treated with oleuropein; **D:** Negative control treated with combination of sitagliptin and oleuropein, all show normal histological structure of rat's renal cortex with the proximal convoluted tubules (P) that are lined with high cuboidal cells with rounded vesicular basal nuclei (arrow) and deeply acidophilic cytoplasm, the distal convoluted tubules (D) have wider lumina and are lined with cubical cells with rounded vesicular central nuclei and paler acidophilic cytoplasm; **E**: Cisplatin treated rats have focal areas of marked tubular degeneration and dilation (DG), atrophied renal proximal and distal tubules with pyknotic and karryorrhetic nuclei (arrowhead); **F** and **G**: Cisplatin+ sitagliptin treated rats and Cisplatin+ oleuropein treated rats respectively, both groups show mild tubular recovery in form of intact cubical tubular cells with rounded vesicular central nuclei. Few tubules show cellular swelling and are having pyknotic nuclei (arrowhead) and hyalin cast (H), **H**: Cisplatin+sitagliptin+oleuropein treated rats show an improvement in tubular structure and minimal cellular swelling.

3.6. Effect of sitagliptin and oleuropein on renal ultrastructure of cisplatin-treated rats

The ultra-structure of the rats' kidneys was shown in **Fig. 5.** The control group **(Fig. 5A)** and negative control **(Fig. 5B-D)**, all showed normal ultra-tubular structure in form of intact tubular cells. Structural abnormalities after cisplatin involved extensive apoptosis with disintegrated cellular components, while autophagy was highly limited. On the other hand, cotreatment with Sita **(Fig. 5E)** or Ole **(Fig. 5F)** resulted in accumulation of autophagosomes. Concurrently, it was observed that a subset of renal tubular cells exhibited various degrees of damage. Combined treatment with Sita and Ole restored renal cells vitality, inhibited vacuolization and resolved autophagic vesicles accumulation **(Fig. 5H)**.

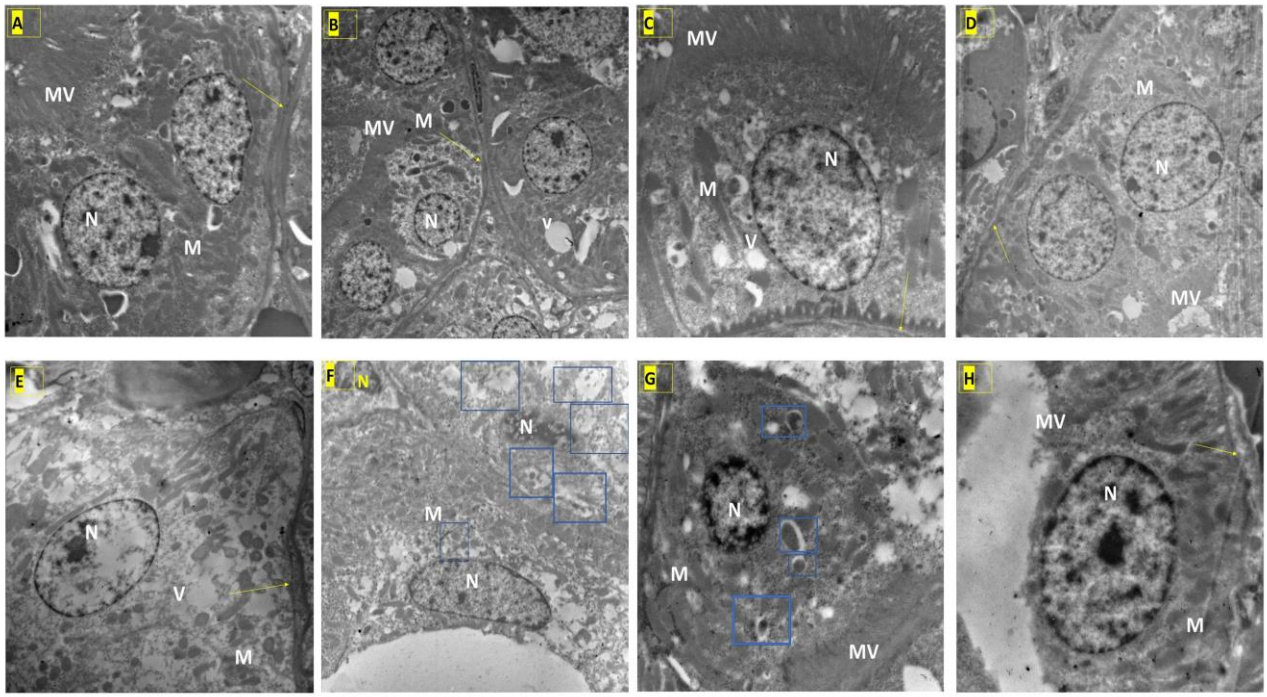

Fig. 5. Ultra structure of renal tubular cells by Transmission Electron Microscopy

A: Control group; **B:** Negative control treated with sitagliptin; **C:** Negative control treated with oleuropein; **D:** Negative control treated with combination of sitagliptin and oleuropein, all show renal tubular cells which are exhibiting long abundant apical microvilli (MV), elongated profuse mitochondria (M), euchromatic nuclei (N), intact basal membrane (arrow), and minimal cytoplasmic vacuolation (V); **E**: In the cisplatin treated rats, the cytoplasm is vacuolated (V), mitochondria are shredded or with disrupted cristae (M), basal lamina is dislocated (arrows), there is loss of of microvilli, and the nucleus (N) shows remnants of nuclear components; **F**: In cisplatin+ sitagliptin treated rats, the renal tubular cells show shrunken nuclei with condensed chromatin that are marginated supportive of apoptotic processes, small sized mitochondria that are irregular in shape and there is accumulation of autophagosomes (square); **G**: In cisplatin+ oleuropein treated rats, the renal tubular cells show shrunken heterochromatic nucleus, swollen mitochondria and multiple autophagosomes (square). **H**: Cisplatin+ sitagliptin+ oleuropein treated rats show tubular cells with normal euchromatic nuclei (N) and electron dense elongated mitochondria (M) and intact microvilli (MV), while autophagosomes and vacuoles are absent.

3.7. Effect of sitagliptin and oleuropein on autophagy, autophagic flux and apoptosis

Further validation of Sita **(Fig. 6A, a-c)** and Ole **(Fig. 6A, d-f)** monotherapy induced autophagic lagging was done by transmission electron microscopy. The count of total autophagosomes per field using electron micrographs showed a significant increase in the number of autophagosomes with Sita and Ole monotherapy **(Fig. 6B)**. To further monitor the autophagic dynamics, protein expression of LC3-II was assessed **(Fig. 7A)**. LC3-II is the most used indicator of autophagy as it is directly correlated with the total number of autophagosomes. Our results showed no significant difference in LC3-II levels among all animal groups except for the cisplatin-intoxicated group which showed marked inhibition of LC3-II levels when compared with the control groups **(Fig. 7A)**.

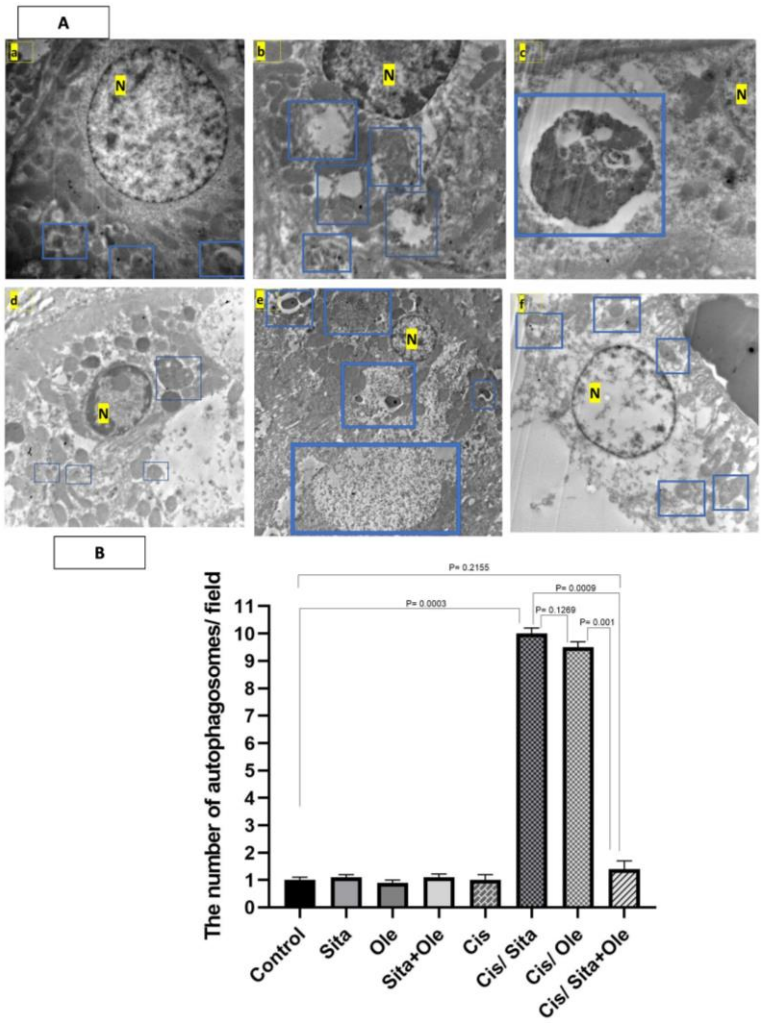

Fig. 6. (A) Electron microscopic analysis of autophagy in the monotherapy with Sita **(a-c)** or OLE **(d-f)**: Selected micrographs show the accumulation of autophagosomes in renal cells, where some autophagosomes are enclosing cytosol others are enveloping organelles. Also, renal cells display varying degree of cellular damage in alignment with the impaired autophagic flux. **(B)** Quantification of autophagosomes. The number of autophagosomes/field was determined in electron micrographs from at least 3 randomly selected visual fields. Data are expressed as means ± S.D.

On the other hand, P62 is an autophagy receptor protein that regulates autophagosomal degradation by acting as a substrate for autophagosomes. Hence, abnormal accumulation of P62 indicates impaired autophagic flux. Our results showed no significant difference in P62 levels amongst the control groups and the cisplatin-intoxicated group. In contrast, sitagliptin treatment showed a significant accumulation of p62 and to a lesser extent in the oleuropein treatment group when compared with the control groups. Our results also showed a significant decrease in P62 levels in the combined-treatment group when compared with the control groups **(Fig 7B)**.

Both levels of LC3-II as an indicator of autophagy, and P62 is an indicator for the autophagic flux, should be jointly interpreted to provide an indication for the autophagy pathway. A concurrent upregulation of both LC3-II and P62 indicates increased autophagosomes albeit impaired autophagic flux as in sita and ole treated groups. In the combined treatment group, LC3-II was significantly increased indicating activated autophagy, while P62 showed no significant difference from the control groups indicating normal autophagic flux.

As caspases are the main executioners of apoptosis that play a central role of cisplatin-induced nephrotoxicity, we evaluated caspase-3 levels through western blot analysis from each experimental group. The cisplatin-intoxicated group showed a high spike in caspase-3 levels indicating renal toxicity compared with the control groups. While cisplatin-intoxicated groups treated with sitagliptin, oleuropein or both showed a significant decrease in caspase-3 levels compared with the non-treatment groups, indicating desirable nephroprotective effects. Notably, caspase-3 levels in the cisplatin-intoxicated group treated with sitagliptin were significantly lower than those of the oleuropein treated group while significantly higher than those of the combination group **(Fig 7C)**.

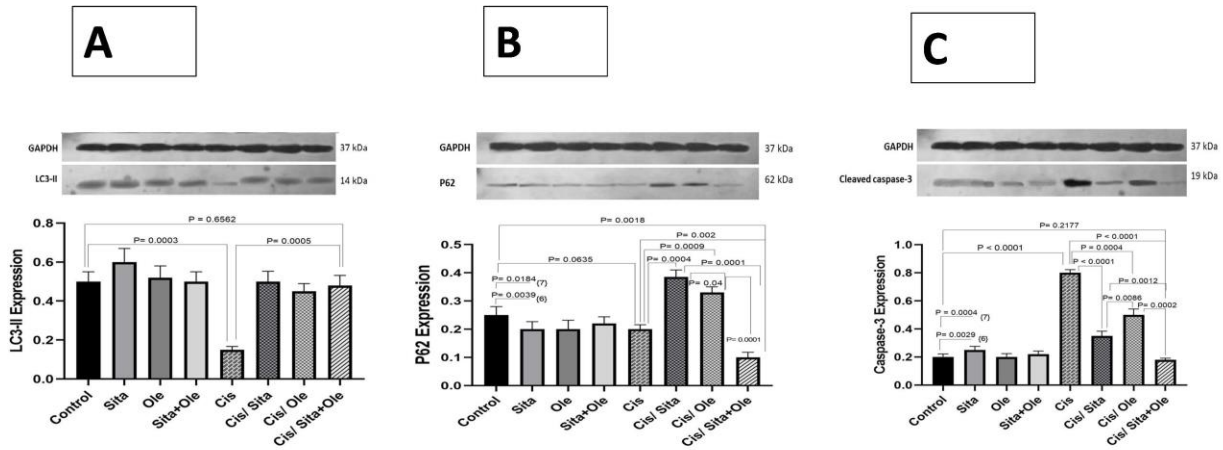

Fig. 7. Effects of cisplatin, Sita and OLE on protein expression of LC3-II **(A)**, P62 **(B)**, and Cleaved caspase-3 **(C)** in renal tissue, as shown by Western blot analysis. Bars represent corresponding protein expression levels relative to GAPDH. Values are expressed as the means ± S.D. $P < 0.05$ is considered statistically significant; one-way ANOVA followed by Bonferroni-corrected post hoc tests were performed.

3.8. Effect of sitagliptin and oleuropein on cisplatin-induced oxidative stress

The antioxidant response element (ARE) is responsible for the regulation of cellular redox balance and protective antioxidant detoxification responses. Nrf2 is a transcription factor that activates a cascade of genes that constitute the antioxidant response element including HO-1 and SOD providing a robust protection against oxidative stress. The cisplatin-intoxicated group showed a significant decrease in the levels of Nrf2 **(Fig 8A)**, HO-1 **(Fig 8B)**, SOD **(Fig 8C)** and a significant increase in MDA **(Fig 8D)** compared with those of the control groups and those of the treatment groups indicating significant oxidative stress. On the other hand, sitagliptin and oleuropein single treatment showed a significant increase in ARE markers and a significant decrease in MDA levels compared with the cisplatin-intoxicated group, but the effect was significantly lower than that of the combined-treatment group and the control groups. There was no significant difference in the levels of Nrf2, HO-1, SOD and MDA between the control groups and the combined-treatment group.

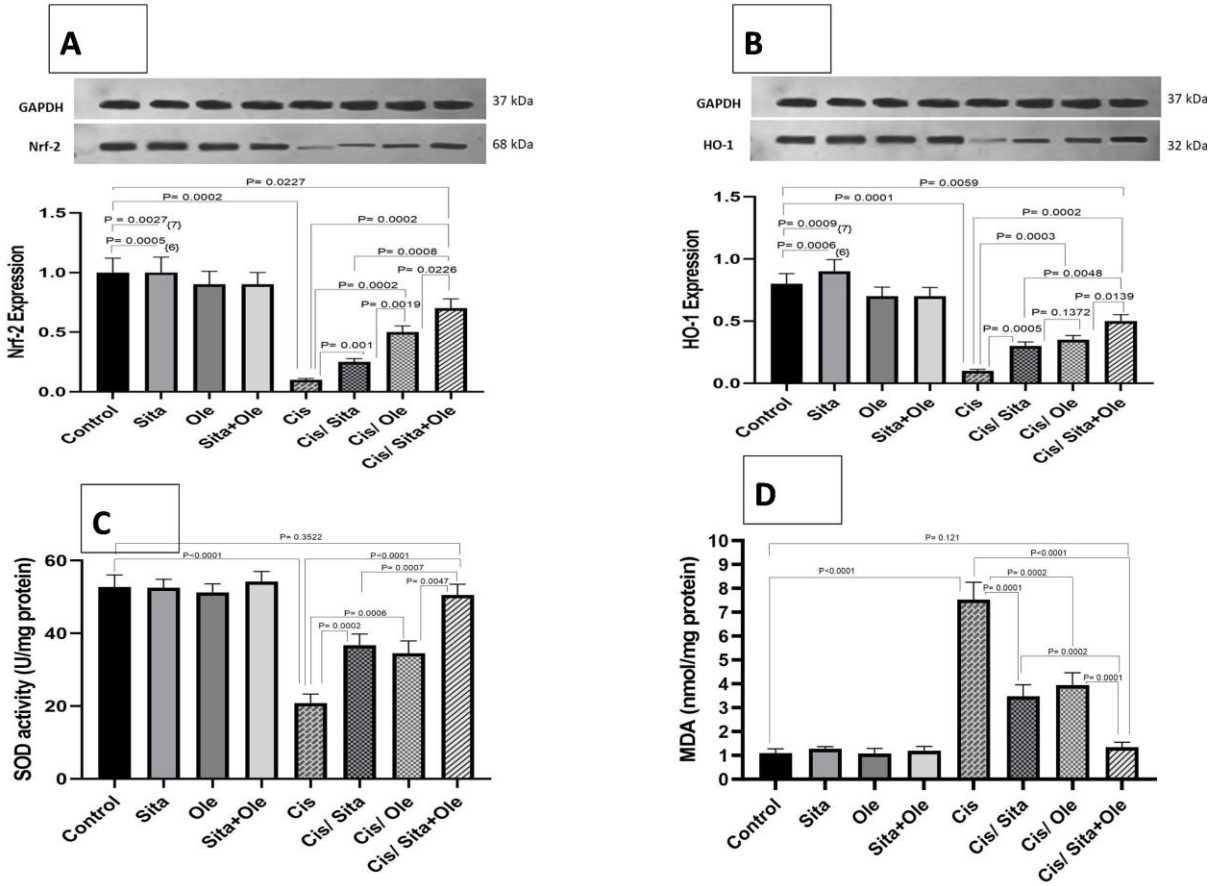

Fig. 8. Effect of sitagliptin and oleuropein on cisplatin-induced oxidative stress; **A:** protein expression of Nrf-2; **B:** protein expression of HO-1 as shown by Western blot analysis in renal tissue, bars represent corresponding protein expression levels relative to GAPDH; **C:** SOD (unit/mg of tissues); **D:** MDA (nmoles per mg tissue). Data are presented as means ± SD. $P < 0.05$ is considered statistically significant; one-way ANOVA followed by Bonferroni-corrected post hoc tests were performed.

4. Discussion

Increasing evidence suggests that after acute injury, the kidney has high capability of repair, yet end-stage renal failure, mortality, or progression to chronic kidney disease present higher probability **[25]**. Such high risk of adverse response to injury mandates identifying the cellular mechanisms that promote renal repair.

Cisplatin-induced AKI is one of the most common experimental models used for assessment of nephroprotective agents **[26]**. In the present study, we assessed the therapeutic potential of Sita, Ole and the combination of these two drugs in cisplatin-induced AKI. In this study, Sita and Ole in monotherapy showed accelerated kidney recovery as shown by the decrease in serum urea, creatinine, and kidney weight compared with the cisplatin-intoxicated untreated group. In AKI, renal tubular swelling and tissue inflammation cause increased kidney weight indicative of tissue damage. However, combined treatment with Sita/ Ole achieved significant renal healing relative to the monotherapy groups, as shown by the significantly decreased kidney weight, serum levels of urea, creatinine, SDF-1α, while enhanced SDF-1α level inside kidney tissues. Mechanistically, the combination group inhibited oxidative stress, apoptosis while activated autophagy of renal tissues through the SDF-1α - Nrf2/HO-1 panel. Interestingly, we found that Sita and Ole in monotherapy application activated the early stages of autophagy as indicated by increased the protein level of LC3-II. Moreover, the monotherapy exhibited increased number of autophagosomes and increased the levels of P62 protein, indicating that the monotherapy was insufficient for completion of the autophagy process and did not offer degradation of autophagosomes for recycling cellular protein. On the other side, the combination use of Sita and Ole resulted in activation of autophagy and in reaching the late stages of autophagy as indicated by increased LC3-II protein levels, meanwhile decreased the number of autophagosomes and the corresponding protein P62.

In the current study, the administration of cisplatin to SD rats in a single dose caused nephrotoxicity evident by significant rise in kidney weight, serum urea and creatinine levels. Parallel to functional failure, histological imaging of the cisplatin group revealed glomerular damage and tubular cell necrosis, conforming with previous studies **[27]**. In pursuing molecular mechanisms, we found that five days after cisplatin toxicity, oxidative stress persisted while antioxidant guardians like SOD and HO-1 were downregulated. It is well known that if oxidative stress is upstream, then cell death is downstream, however functional autophagy exhibits a hope on the horizon as a survival alternative **[28]**. Autophagy can brush off incompetent cellular composites, thereby attenuating the oxidative damage of macromolecules, while recycling them to meet the high energy needs **[29]**. In this study, we found that cisplatin-intoxicated rats had significant increase in the levels of caspase-3, indicating active apoptosis. We found diminished levels of LC3-II and P62 implying inactive autophagy. Cisplatin has been extensively reported as an inducer of autophagy **[21]**, yet it is still unclear as to how early autophagy remains induced. Several studies indicated that autophagy was induced in the first few hours after cisplatin treatment **[30]**. However, the results here, along with others [**31]**, clarified that as the days elapsed, autophagy turned inactive.

Therefore, there is an increasing interest in pharmacological agents that induce autophagy. The autophagic process involves building double-membrane structures, termed autophagosomes, in the cytoplasm to encompass damaged proteins

and cell organelles **[29]**. Autophagosomes are then fused with lysosomes forming autophagic vacuoles or autophagolysosomes which digest cellular ruins into essential metabolites **[32]**. Recently, considerable studies have reported that Sita, a hypoglycemic drug, has tissue protective functions via induction of autophagy **[33]**. We propose that Sita activates autophagy by avoiding the degradation of the renal tissue level of SDF-1α.

In the cisplatin group, we found that serum levels of SDF-1α were highly upregulated. Recently, serum levels of SDF-1α were found elevated in patients with cardiovascular disease and end stage renal failure **[34]**. Injury-induced upregulation of serum SDF-1α is believed to be a compensatory mechanism to regulate trafficking of stem cells during insult **[35]**, thus is highly implicated in reparation of cisplatin-induced AKI. In the Sita groups, serum levels of SDF-1α were significantly lower than their counterparts in the cisplatin group which suggests a lesser magnitude of damage.

On the other hand, tissue levels of SDF-1α were found to be upregulated in the Sita, opposite to their serum levels and to the tissue levels in the cisplatin group. This discrepancy can be interpreted as serum SDF-1α is upregulated in cisplatin-induced AKI to facilitate homing of stem cells to the kidney tissues, but it is subjected to degradation by the DPP-4. Hence, the use of Sita, a DPP-4 inhibitor, enhanced renal SDF-1α levels. Earlier, increased renal SDF-1α expression slowed the progression of renal decline in CKD **[36]**. Critically, SDF-1α has been proven to promote tissue regeneration by triggering the autophagy process and inhibiting apoptosis **[37]**.

In the Sita group, we observed an attenuation of the apoptotic process as reflected by the significantly decreased caspase-3 expression levels. We also found that Sita group had elevated levels of LC3-II, marking autophagosome formation and the induction of early steps of autophagy. On the other hand, upregulated P62 levels in Sita group shows the impediment of autophagosome clearance **[38]**. Ultrastructural imaging of the sita group showed accumulation of autophagosomes in tubular cells. We also found elevated levels of MDA indicating persistent oxidative stress in renal cells of the sita group which is proposed to be primed by the imbalance of autophagic flux **[39]**. Histopathological analysis of the sita group confirmed that a significant proportion of tubular cells was disrupted, aligned with interrupted autophagic pathway. In tandem with high renal levels of SDF-1α, we found intact glomerular structure. Previously, SDF-1α was viewed to conserve microvascular integrity and improve vasculogenesis in renal failure **[36].** Moreover, SDF-1α overexpression was postulated to guide endothelial progenitor cells to injured tissues to participate in the neogenesis of vascularization **[40]**.

Together, these findings suggest that high renal level of SDF-1α, via restoring renal vasculature and improving blood flow, provided the energy requirements which subsequently inhibited apoptotic cell death and activated autophagy. Since apoptosis is a faster process than autophagy **[41]**, it is plausible that SDF-1α renal levels were insufficient to follow through the late stage of autophagy. This is expected to expose renal cells to fatality due to failure of autophagy- elicited cell survival [**42]**.

Moreover, we gave special concern to the impact of sita on Nrf2/HO-1 axis since it has been implicated in the SDF-1α /CXCR4 signaling pathway **[43]**. HO-1 is a powerful redox-sensitive enzyme for which, Nrf2 is a basic leucine zipper transcription factor **[44]**. The interplay between SDF-1α/CXCR4 and Nrf2/HO-1 signaling pathway is beyond the classic antioxidant role of

Nrf2/HO-1, as Nrf2/HO-1 has been shown to consolidate the functionality of SDF-1α **[45]**. Our data demonstrate that sita induced Nrf2/HO-1 expression. The ability of SDF-1α to induce the expression of Nrf2/HO-1 is a novel finding in recent research **[46]**.

This led us to study combining Sita with agents that have the potential to target these pathways, therefore potentiating the remedial outcome. Mounting evidence acknowledged that Ole is a potent antioxidant agent and a scavenger for free radicals. Its antioxidant properties are mainly through the activation of the Nrf2 pathway and the subsequent HO-1 enzyme which is pivotal in the protection of cellular macromolecules from oxidative stress and cisplatin-induced renal damage. The present results indicate that Ole pretreatment improved the typical markers of renal dysfunction and bettered the tubular lesion. Ole decreased serum levels of SDF-1α, an indication of recovery effects. Pre-treatment with ole in our study produced upregulation of the expression of Nrf2/HO-1. Still, renal levels of SDF-1α in response to ole were decreased, which translated into visible glomerular damage. This is expected to interrupt the SDF-1α/Nrf2/HO-1 panel. On the other hand, apoptosis was remarkably active, autophagy was lagging, and oxidative stress was aggravated after ole treatment.

Coadministration of Sita/Ole corrected the negative effects of cisplatin on renal parameters. The use of Sita/Ole combination showed augmentation of Nrf2/HO-1 expression compared with the monotherapy groups. Interestingly, an amplification of renal levels of SDF-1α was shown even though the effect of ole monotherapy was insignificant. It was recently reported that HO-1 upregulated the expression level of SDF-1α **[47]**.

This raises the query of whether SDF-1α/Nrf2/HO-1 panel in the cisplatin/Sita+Ole group is employed to serve cell survival through suppression of apoptosis and induction of autophagy. Our data verified that combined use of Sita/Ole resulted in ceasing of apoptosis. Interestingly, the combined Sita/Ole significantly increased the expression of LC3-II and decreased the expression of P62 relative to the monotherapy groups, indicating the eliminating of the autophagic cargo. In response to the above settings, oxidative stress was significantly decreased indicating a high extent of repair. These actions clearly had positive effects on renal architecture, as manifested by intact glomeruli and vital renal tubular cells.

A key question that may arise is as to whether GLP-1, the primary substate for DPP4, is implicated in the renal functional and structural damage induced by cisplatin. Initial analysis by ELISA revealed that GLP-1 levels in renal tissues of cisplatin group was insignificantly different from the control group. Furthermore, it was shown that sita could increase GLP-1 renal levels. We speculated whether GLP-1 is linked to combined Sita/Ole induced alleviation of renal functional and structural damage. In contrast, we found that combined Sita/Ole had no significant effect on GLP-1 levels relative to both the control and cisplatin groups. The above data indicate that the protective renal effects of combined Sita/Ole are mainly through the action of SDF-1α inside renal cells.

Conclusion

In conclusion, we found that the key aspects of Sita renal protection is an anticipatory redistribution and trafficking of SDF-1α to injured renal cells followed by inhibition of SDF-1α proteolytic cleavage. This pattern of distribution suggests increased serum SDF-1α levels as a marker of renal damage while elevated renal SDF-1α levels as a marker of repair. Furthermore, the action of Sita was remarkably enhanced after using Ole in combination. These

outcomes suggest that the combined use of Sita/Ole in Cisplatin-induced AKI increased SDF-1α in renal tissue, leading to Nrf2/HO-1 overexpression, leading to the activation of a complete autophagic pathway.

Abbreviations

AKI, acute kidney injury; ALT, alanine aminotransferase; AST, aspartate aminotransferase; DPP, dipeptidylpeptidase-4; GLP-1, glucagon-like peptide-1; H&E, hematoxylin and eosin; HO-1, heme oxygenase-1; MDA, malondialdehyde; Nrf2, nuclear factor-erythroid 2-related factor 2; Ole, oleuropein; Sita, sitagliptin; SDF-1α, stromal cell-derived factor-1; SOD, superoxide dismutase.

Declarations

Ethics approval and consent to participate

This study was approved by Research Ethics Committee of the Faculty of Pharmacy, Ain Shams University (Approval No. 271-24/11/2019).

Consent to publish

Not applicable

Availability of data and materials

All data generated or analyzed during this study are included in the main manuscript. Competing interests

Authors have no competing interests to be declared.

Funding statement

This research did not receive any funding from any agencies.

5. References

1- Fang Y., Ding X., Zhong Y. Acute kidney injury in a Chinese hospitalized population. Blood Purif. 2010; 30:120–126.

2- Lafrance J., Miller D. Acute kidney injury associates with increased long-term mortality. J Am Soc Nephrol. 2010; 21:345–352.

3- Schrier R., Wang W., Poole B., Mitra A. Acute renal failure: definitions, diagnosis, pathogenesis, and therapy. J Clin Invest. 2004; 114:5–14.

4- Bao YW, Yuan Y, Chen JH, Lin WQ. Kidney disease models: tools to identify mechanisms and potential therapeutic targets. Zool Res. 2018 Mar 18;39(2):72-86.

5- Dasari S, Tchounwou PB. Cisplatin in cancer therapy: molecular mechanisms of action. Eur J Pharmacol. 2014; 740:364-78.

6- Ciarimboli G. Membrane transporters as mediators of Cisplatin effects and side effects. Scientifica. 2012; 2012:473829.

7- Jiang M, Wang CY, Huang S, Yang T, Dong Z. Cisplatin-induced apoptosis in p53-deficient renal cells via the intrinsic mitochondrial pathway. American Journal of Physiology-Renal Physiology. 2009; 296(5): F983-993.

8- Kodama A, Watanabe H, Tanaka R, Kondo M, Chuang VT, Wu Q, Endo M, Ishima Y, Fukagawa M, Otagiri M, Maruyama T. Albumin fusion renders thioredoxin an effective anti-oxidative and anti-inflammatory agent for preventing cisplatin-induced nephrotoxicity. Biochimica et Biophysica Acta. 2014; 1840(3):1152-62.

9- Ozkok A, Edelstein CL. Pathophysiology of cisplatin-induced acute kidney injury. Biomed Res Int. 2014; 2014: 967826.

10- Gong L, Pan Q, Yang N. Autophagy and Inflammation Regulation in Acute Kidney Injury. Front Physiol. 2020; 11: 576463.

11- He L, Livingston MJ, Dong Z. Autophagy in acute kidney injury and repair. Nephron Clin Pract. 2014;127(1-4):56-60.

12- Demuth HU, McIntosh CH, Pederson RA. Type 2 diabetes–therapy with dipeptidyl peptidase IV inhibitors. *Biochim Biophys Acta* (2005) 1751:33–44.

13- Yu DM, Yao TW, Chowdhury S, Nadvi NA, Osborne B, Church WB, et al. The dipeptidyl

peptidase IV family in cancer and cell biology. *FEBS J.* (2010) 277:1126–44.

14- Ren X, Zhu R, Liu G, Xue F, Wang Y, Xu J, Zhang W, Yu W, Li R. Effect of sitagliptin on tubulointerstitial Wnt/β-catenin signalling in diabetic nephropathy. Nephrology (Carlton). 2019;24(11):1189-1197.

15- Shi W, Zhang D, Wang L, Sreeharsha N, Ning Y. Curcumin synergistically potentiates the protective effect of sitagliptin against chronic deltamethrin nephrotoxicity in rats: Impact on pro-inflammatory cytokines and Nrf2/Ho-1 pathway. J Biochem Mol Toxicol. 2019; 33(10): e22386.

16- Deacon CF. Peptide degradation and the role of DPP-4 inhibitors in the treatment of type 2 diabetes. Peptides. 2018; 100:150-157.

17- Ho TK, Shiwen X, Abraham D, Tsui J, Baker D. Stromal-Cell-Derived Factor-1 (SDF-1)/CXCL12 as Potential Target of Therapeutic Angiogenesis in Critical Leg Ischaemia. Cardiol Res Pract. 2012; 2012:143209.

18- Sun Z, Li X, Zheng X, Cao P, Yu B, Wang W. Stromal cell-derived factor-1/CXC chemokine receptor 4 axis in injury repair and renal transplantation. J Int Med Res. 2019; 47(11): 5426-5440.

19- Angeloni C, Malaguti M, Barbalace MC, Hrelia S. Bioactivity of Olive Oil Phenols in Neuroprotection. Int J Mol Sci. 2017; 18(11): 2230.

20- Lin HH, Chen YH, Chang PF, Lee YT, Yet SF, Chau LY. Heme oxygenase-1 promotes neovascularization in ischemic heart by coinduction of VEGF and SDF-1. J Mol Cell Cardiol. 2008; 45(1): 44 55.

21- Lin JF, Lin YC, Tsai TF, Chen HE, Chou KY, Hwang TI. Cisplatin induces protective autophagy through activation of BECN1 in human bladder cancer cells. Drug Des Devel Ther. 2017; 11:1517-1533.

22- Li, Y., Zheng, M., Sah, S.K., Mishra, A. and Singh, Y. Neuroprotective influence of sitagliptin against cisplatin-induced neurotoxicity, biochemical and behavioral alterations in Wistar rats. Mol Cell Biochem. 2019; 455: 91–97

23- Jemai H, El Feki A, Sayadi S. Antidiabetic and antioxidant effects of hydroxytyrosol and oleuropein from olive leaves in alloxan-diabetic rats. J Agric Food Chem. 2009; 57(19): 8798-804.

24- Suddek GM. Sunitinib improves chemotherapeutic efficacy and ameliorates cisplatin-induced nephrotoxicity in experimental animals. Cancer Chemother Pharmacol. 2011; 67(5): 1035-44.

25- Chawla LS, Eggers PW, Star RA, Kimmel PL. Acute kidney injury and chronic kidney disease as interconnected syndromes. The New England Journal of Medicine. 2014; 371(1): 58–66.

26- Singh AP, Junemann A, Muthuraman A, Jaggi AS, Singh N, Grover K, Dhawan R. Animal models of acute renal failure. Pharmacol Rep. 2012; 64(1):31-44.

27- Terada Y, Inoue K, Matsumoto T, Ishihara M, Hamada K, Shimamura Y, Ogata K, Inoue K, Taniguchi Y, Horino T, Karashima T, Tamura K, Fukuhara H, Fujimoto S, Tsuda M, Shuin T. 5-Aminolevulinic acid protects against cisplatin-induced nephrotoxicity without compromising the anticancer efficiency of cisplatin in rats in vitro and in vivo. PLoS One. 2013; 8(12): e80850.

28- Filomeni G, De Zio D, Cecconi F. Oxidative stress and autophagy: the clash between damage and metabolic needs. Cell Death Differ. 2015; 22(3): 377-388.

29- Galluzzi L, Pietrocola F, Levine B, Kroemer G. Metabolic control of autophagy. Cell. 2014; 159(6): 1263-76.

30- Yang C, Kaushal V, Shah SV, Kaushal GP. Autophagy is associated with apoptosis in cisplatin injury to renal tubular epithelial cells. Am J Physiol Renal Physiol. 2008; 294(4): F777-87.

31- Wu J, Zheng C, Wan X, Shi M, McMillan K, Maique J, Cao C. Retinoic Acid Alleviates Cisplatin-Induced Acute Kidney Injury Through Activation of Autophagy. Front Pharmacol. 2020; 11:987.

32- Zhifen Yang, Daniel J Klionsky, Mammalian

autophagy: core molecular machinery and signaling regulation, Current Opinion in Cell Biology. 2010; 22(2): 124-131.

33- Zhou Y, Wang H, Man F, Guo Z, Xu J, Yan W, Li J, Pan Q, Wang W. Sitagliptin Protects Cardiac Function by Reducing Nitroxidative Stress and Promoting Autophagy in Zucker Diabetic Fatty (ZDF) Rats. Cardiovasc Drugs Ther. 2018; 32(6): 541-552.

34- Mousavi SH, Dormanesh B, Shahidi S, Johari Moghadam A, Kazemi M, Abediny A. Stromal Cell-derived Factor-1 and CXC Chemokine Receptor Type-4 are Associated with Cardiovascular Disease in Patients under Hemodialysis. Int J Prev Med. 2019; 10: 219.

35- Cheng M, Huang K, Zhou J, Yan D, Tang YL, Zhao TC, Miller RJ, Kishore R, Losordo DW, Qin G. A critical role of Src family kinase in SDF-1/CXCR4- mediated bone-marrow progenitor cell recruitment to the ischemic heart. J Mol Cell Cardiol. 2015; 81: 49–53.

36- Chen LH, Advani SL, Thai K, Kabir MG, Sood MM, Gibson IW, Yuen DA, Connelly KA, Marsden PA, Kelly DJ, Gilbert RE, Advani A. SDF-1/CXCR4 signaling preserves microvascular integrity and renal function in chronic kidney disease. PLoS One. 2014; 9(3): e92227.

37- Yang JW, Zhang YF, Wan CY, Sun ZY, Nie S, Jian SJ, Zhang L, Song GT, Chen Z. Autophagy in SDF-1α-mediated DPSC migration and pulp regeneration. Biomaterials. 2015; 44: 11-23.

38- Yoshii SR, Mizushima N. Monitoring and measuring autophagy. Int J Mol Sci. 2017; 18: 1865.

39- Ornatowski W, Lu Q, Yegambaram M, Garcia AE, Zemskov EA, Maltepe E, Fineman JR, Wang T, Black SM. Complex interplay between autophagy and oxidative stress in the development of pulmonary disease. Redox Biol. 2020; 36: 101679.

40- Si XY, Li JJ, Yao T, Wu XY. Transforming growth factor-β1 in the microenvironment of ischemia reperfusion-injured kidney enhances the chemotaxis of mesenchymal stem cells to stromal cell-derived factor-1 through upregulation of surface chemokine (C-X-C motif) receptor 4. Mol Med Rep. 2014; 9: 1794–1798.

41- Thorburn J, Andrysik Z, Staskiewicz L, Gump J, Maycotte P, Oberst A, Green DR, Espinosa JM, Thorburn A. Autophagy controls the kinetics and extent of mitochondrial apoptosis by regulating PUMA levels. Cell Rep. 2014; 7(1): 45-52.

42- Noguchi T, Suzuki M, Mutoh N, Hirata Y, Tsuchida M, Miyagawa S, Hwang GW, Aoki J, Matsuzawa A. Nuclear-accumulated SQSTM1/p62-based ALIS act as microdomains sensing cellular stresses and triggering oxidative stress-induced parthanatos. Cell Death Dis. 2018; 9(12): 1193.

43- Yu G, Liu P, Shi Y, Li S, Liu Y, Zhu W. Sitagliptin Stimulates Endothelial Progenitor Cells to Induce Endothelialization in Aneurysm Necks Through the SDF-1/CXCR4/NRF2 Signaling Pathway. Front Endocrinol *(Lausanne)*. 2019; 10: 823.

44- Moi P, Chan K, Asunis I, Cao A, Kan YW. Isolation of NF-E2-related factor 2 (Nrf2), a NF-E2-like basic leucine zipper transcriptional activator that binds to the tandem NF-E2/AP1 repeat of the beta-globin locus control region. Proc Natl Acad Sci USA. (1994) 91:9926–30.

45- Deshane J, Chen S, Caballero S, Grochot-Przeczek A, Was H, Li Calzi S, Lach R, Hock TD, Chen B, Hill-Kapturczak N, Siegal GP, Dulak J, Jozkowicz A, Grant MB, Agarwal A. Stromal cell-derived factor 1 promotes angiogenesis via a heme oxygenase 1-dependent mechanism. J Exp Med. 2007; 204(3): 605-18.

46- Jin W, Zhao Y, Hu Y, Yu D, Li X, Qin Y, Kong D, Wang H. Stromal Cell-Derived Factor-1 Enhances the Therapeutic Effects of Human Endometrial Regenerative Cells in a Mouse Sepsis Model. Stem Cells Int. 2020; 2020: 4820543.

47- Wei G, Yin Y, Duan J, Guo C, Zhu Y, Wang Y, Xi M, Wen A. Hydroxysafflor yellow A promotes neovascularization and cardiac function recovery through HO-1/VEGF-A/SDF-1α cascade. Biomed Pharmacother. 2017; 88: 409-420.